京都大学防災研究所年報　第 54 号 B　平成 23 年 6 月
Annuals of Disas. Prev. Res. Inst., Kyoto Univ., No. 54 B, 2011

Numerical Analysis of Flooding Impacts Using Hydro-BEAM in Red River Basin, Vietnam

Mukta SAPKOTA*, Toshio HAMAGUCHI and Toshiharu KOJIRI

* Graduate School of Engineering, Kyoto University

Synopsis

Flood hazard is one of the most harmful disasters in the world. It is significant to obtain reliable information on flood characteristics for flood hazard mitigation. In this study, a simplified flood inundation model integrated with hydrological model Hydro-BEAM (Hydrological River Basin Environmental Assessment Model) has been developed to analyze the flood characteristics and identify the flood hazard area. The study outlines the development of a typical model of inundating flow which is a composite model of building and water conduction in space. Developed model has been used for flood inundation simulation in Hanoi, Vietnam.

Keywords: Hydro-BEAM, flood inundation, moving boundary

1. Introduction

Natural disasters have an impact on people, property, society, and the environment at an alarming rate. The number of people affected by natural disasters averaged 125 million per year during 1980-1989, which increased to 203 million per year during 1990-1999 and then to 234 million per year during 2000-2009. Flooding was responsible for half of these affected and caused over one-fourth of the total estimated economic damage. An effective flood modeling and prediction system could help mitigate the worst effects of flood disasters through the rapid dissemination of information in areas under threat. Hence, it is significant to obtain information on flood characteristics, study the hydrological system and simulating different extreme events to visualize the probable floods that would exceed the flood control design standards for disaster mitigation. Flood hazard maps can be a tool to communicate about flooding problem in the region and enhance the awareness of people. This could help community to be proactive and prepared towards such events and reduce loss from flood disaster.

South-east Asia is one of the most frequently affected regions by flood. Many of the cities in these regions are vulnerable to floods due to their geographic locations in floodplain of large rivers (Dutta and Herath, 2004). Hanoi, the capital of Vietnam, is one of such cities, which is located in the Red River delta with average elevation less than 20m and highly vulnerable to flood (Tran et al., 2007). The problem has been compounded in recent years by a number of changes, such as environmental degradation, global climate change, sedimentation and degradation of the existing extensive system of dykes (Hansson and Ekenberg, 2002).

This research develops a distributed model for simulating flood inundation integrating with rainfall-runoff processes. Various hydrologic models, especially commercial software, have been developed in the past to simulate flood inundation. Whilst existing 2D flood models are good at simulating urban inundation processes, the cost is too high. Also, in such models, whole basin is divided into small meshes and calculation is done at each single mesh, with detailed behavior. To describe the apparent flooding behavior, detailed flooding limits surface water fluctuation is not required. Considering this, a model which can follow water depth transfers has been developed.

2. Study Area

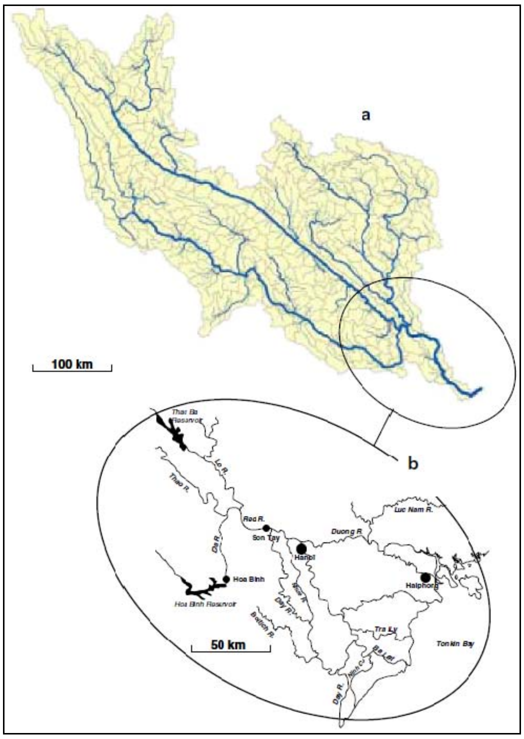

Fig. 1 Map of the Red River Basin (a) its three major upstream tributaries and (b) its delta area

Hanoi City is located in the flood plain of red river basin (Fig. 1) which is situated in South East Asia (from 20°00' to 25°30' North; from 100°00' to 107°10' East) and drains an area of 156,451 km^2, of which 50.3% in Vietnam, 48.8% in China and 0.9% in Laos (Le et al., 2007). The city is situated at latitudes 20°53' - 21°23' N and longitudes 105°44' - 106°02' E (Tran et al., 2007).

3. Model Development

3.1 Hydrological Model

A physically-based distributed hydrological model, Hydro-BEAM (Hydrological River Basin Environment Assessment Model) has been used for rainfall runoff simulation. The model consists of grid cells with DEM (Digital Elevation Model) and four soil layers (Kojiri et al., 2008). The lateral flow from soil layers A, B and C except D (Fig. 2) can discharge into the river, and the soil moisture can move up and down among the four layers with a no-flux boundary condition at the base of layer D. The model also represents the hydrologic processes of evapotranspiration, runoff from paddy fields, surface runoff, ground water flow, and flow routing in channel and intake/ release. For considering the variations of infiltration due to the land cover changes, five types of land cover are defined in the model. They are mountainous areas, paddy fields, dry fields, urban lands and water-body surfaces.

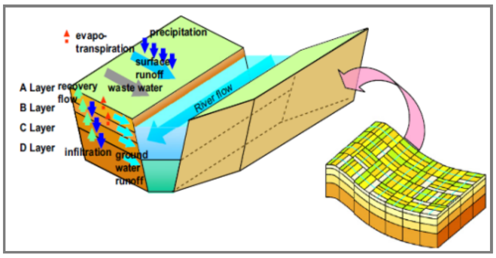

Fig. 2 Schematic structure of Hydro-BEAM

Thornthwaite method has been used to calculate actual evapotranspiration in the model as follows:

$$E_p = 0.553 D_o \left({10T_i}/{J} \right)^a \tag{1}$$

$$a = 0.000000675J^3 - 0.0000771J^2 + 0.1792J + 0.049293 \tag{2}$$

$$J = \sum_{i=1}^{12} \left({T_i}/{5} \right)^{1.514} \tag{3}$$

$$E_a = M.E_p \tag{4}$$

Where E_p is the potential evapotranspiration at month i(mm/day), and D_o is the feasible sunshine duration (h/12h).a and J are the power index and a heat parameter, and are computed using Eq. 2 and 3, respectively. T_i is the monthly averaged temperature at month i (˚C). E_a is the actual evapotranspiration (mm/day), and M is a parameter for representing available moisture vapor.

The linear storage model is used to find the subsurface water in the target area (Eq. 5 and Eq. 6).

$$\frac{dS}{dt} = I - O \tag{5}$$

$$O = (k_1 + k_2)S \tag{6}$$

Where, I and O are input and output discharges, respectively; S is storage; k_1 and k_2 are tank coefficients.

Complex tank model has been used to simulate the runoff process in paddy field. Diffusive wave approximation is used for flow routing.

3.2 Flow Model

The most widely used approach to modeling fluvial hydraulics has been 1D finite difference solutions of the full Saint-Venant Equations (Bates and De Roo, 2000). Eq. 7 represents mass conservation equation (continuity equation) while Eq.8 momentum equation.

$$\frac{\partial Q}{\partial x} + \frac{\partial A}{\partial t} - r_e = 0 \tag{7}$$

$$\frac{1}{A}\frac{\partial Q}{\partial t} + \frac{1}{A}\frac{\partial}{\partial x}\left(\frac{Q^2}{A}\right) + g\frac{\partial y}{\partial x} - g(S_o - S_f) = 0 \tag{8}$$

Where, t is time; x is distance along the longitudinal axis of the water course; A is cross-sectional area; Q is discharge through A; q is lateral inflow or outflow distributed along the x-axis of the watercourse; g is gravity acceleration constant; h is water surface level with reference to datum; S_o is bed slope and S_f is friction slope.

$$g\frac{\partial y}{\partial x} - g(S_o - S_f) = 0 \tag{9}$$

The friction slope can be estimated by Manning’s formula (Eq.10). Bed slope can be estimated by Eq. 11.

$$S_f = \frac{n^2 Q|Q|}{A^2 R^{4/3}} \tag{10}$$

$$S_o = -\frac{\partial z}{\partial x} = -\frac{\partial\left(h - y\right)}{\partial x} \tag{11}$$

Where, n is Manning's roughness coefficient; R is hydraulic radius.

Diffusive wave approximation: In the diffusive wave approximation of Saint Venant’s equations, the local and convective terms in the momentum equation (the first two terms in Eq. 8) are neglected. Thus Eq. 8 will be simplified as:

$$S_f = -\frac{\partial h}{\partial x} \tag{12}$$

Combining Eq. 8 and Eq. 12 yields,

$$Q = \frac{1}{n} R^{2/3} A \frac{-\frac{\partial h}{\partial x}}{\left|\frac{\partial h}{\partial x}\right|^{1/2}} \tag{13}$$

Finite difference equations: A fully implicit finite difference scheme is used to solve these non-linear partial differential equations. Using finite difference scheme, Eq. 7 and Eq. 13 can be expressed as,

$$\frac{A_i^{t+1} - A_i^t}{\Delta t} + \frac{Q_{i+1}^{t+1} - Q_i^{t+1}}{\Delta x} = \frac{r_{ei}^{\ t+1} + r_{ei}^{\ t}}{2} \tag{14}$$

$$Q_i^{t+1} = \frac{1}{n_i} A_i^{t+1} \left(R_i^{t+1}\right)^{2/3} \frac{\frac{h_{i+1}^{t+1} - h_i^{t+1}}{\Delta x}}{\left|\frac{h_{i+1}^{t+1} - h_i^{t+1}}{\Delta x}\right|^{1/2}} \tag{15}$$

3.3 Inundation Model

The proposed inundation model is a composite model of building and water conduction in space, in other words, water depth transfers in porous spaces. So we can consider inundating flow as water depth transfers.

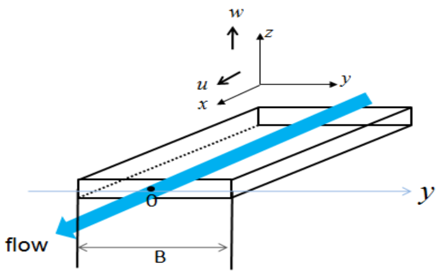

Fig. 3 Flow representation in a mesh

Navier- Stokes equation has been used here for the analysis.

$$\frac{Du}{Dt} = -\frac{1}{\rho}.\frac{\partial p}{\partial x} + \frac{\mu}{\rho}\nabla^2 u \qquad (16)$$

$$\frac{Dw}{Dt} = -\frac{1}{\rho}.\frac{\partial p}{\partial z} - g + \frac{\mu}{\rho}\nabla^2 w \qquad (17)$$

Where, $\frac{D}{Dt} = \frac{\partial}{\partial t} + u\frac{\partial}{\partial x} + v\frac{\partial}{\partial y} + w\frac{\partial}{\partial z}$; u and w are velocities in X- and Z- directions (Fig. 3); ρ and μ are density and viscosity of water; g is acceleration due to gravity; p is water pressure; $\nabla^2 = \frac{\partial^2}{\partial x^2} + \frac{\partial^2}{\partial y^2} + \frac{\partial^2}{\partial z^2}$.

The full 3D Navier-Stokes equations are computationally intensive process. 2D equations are computationally manageable and provide acceptable results (Piotrowski 2010). Also, viscosity of water can be neglected and height of water can be assumed to be not varying during a time step. This simplified scheme is shallow water equation. Furthermore, the advection terms $u\frac{\partial u}{\partial x} + v\frac{\partial u}{\partial y}$, $u\frac{\partial v}{\partial x} + v\frac{\partial v}{\partial y}$ can be ignored assuming the fluid velocity is small. This assumption simplifies the Eq. 16 and Eq. 17 as:

$$\frac{\partial u}{\partial t} = -\frac{1}{\rho}.\frac{\partial p}{\partial x} + \frac{\mu}{\rho}\frac{\partial^2 u}{\partial y^2} \qquad (18)$$

$$\frac{\partial w}{\partial t} = -\frac{1}{\rho}.\frac{\partial p}{\partial z} + \frac{\mu}{\rho}\frac{\partial^2 v}{\partial y^2} \qquad (19)$$

Considering $\frac{\partial u}{\partial t} \approx 0, \frac{\partial w}{\partial t} \approx 0$, Eq. 18 and Eq. 19 become:

$$u = -\frac{\partial p}{\partial x}.\frac{1}{2\mu}\left(\frac{B^2}{4} - y^2\right) \qquad (20)$$

$$w = -\left(\frac{\partial p}{\partial z} + \rho g\right).\frac{1}{2\mu}\left(\frac{B^2}{4} - y^2\right) \qquad (21)$$

Cross sectional mean velocities will be:

$$u_m = \frac{1}{B}\int_{-B/2}^{B/2} u dy = -\frac{B^2}{12\mu}.\frac{\partial p}{\partial x} \qquad (22)$$

$$w_m = \frac{1}{B}\int_{-B/2}^{B/2} w dy = -\frac{B^2}{12\mu}.\left(\frac{\partial p}{\partial z} + \delta g\right) \qquad (23)$$

As, $h = z + \frac{p}{\rho g}$ Eq. 22 and Eq. 23 simplifies to Eq. 24 and Eq. 25 which are similar to Darcy law.

$$u_m = -\frac{\rho g B^2}{12\mu}.\frac{\partial h}{\partial x} \qquad (24)$$

$$w_m = -\frac{\rho g B^2}{12\mu}.\frac{\partial h}{\partial z} \qquad (25)$$

Hence continuity equation is represented by Eq. 26 while momentum equations in X- and Y-direction are represented by Eq. 27 and Eq. 28 respectively.

$$\frac{\partial h}{\partial t} + \frac{\partial (uh)}{\partial x} + \frac{\partial (vh)}{\partial y} \qquad (26)$$

$$\frac{\partial (uh)}{\partial t} + \frac{\partial \left(u^2 h\right)}{\partial x} + \frac{\partial \left(uvh\right)}{\partial y} + gh\frac{\partial h}{\partial x} = -\frac{gnu\sqrt{u^2 + v^2}}{h^{1/3}} \qquad (27)$$

$$\frac{\partial(vh)}{\partial t}+\frac{\partial(uvh)}{\partial x}+\frac{\partial(v^2h)}{\partial y}+gh\frac{\partial h}{\partial y} = -\frac{gnv\sqrt{u^2+v^2}}{h^{1/3}} \quad (28)$$

Designating the ratio of building as λ, continuity and momentum equations can be expressed as:

$$(1-\lambda)\frac{dh}{dt}=-\frac{\partial}{\partial x}(u_m h)-\frac{\partial}{\partial y}(v_m h)+r_e \quad (29)$$

$$u_m=-\kappa_x\frac{\partial h}{\partial x},\quad v_m=-\kappa_y\frac{\partial h}{\partial y} \quad (30)$$

$$\therefore(1-\lambda)\frac{dh}{dt}=\frac{\partial}{\partial x}\left(\kappa_x h\frac{\partial h}{\partial x}\right)+\frac{\partial}{\partial y}\left(\kappa_y h\frac{\partial h}{\partial y}\right)+r_e \quad (31)$$

Here Eq. 31 is very much similar to ground water model.

Researchers can consider the conventional model in picking up only water conduction area as housing/building intervals, gardens, parks and roads. The conventional one can consider detailed behavior of inundating water. The proposed model cannot express water behavior at any points, but it can follow depth transfer (water-quantity movement). In terms of the edges (moving boundaries), we can numerically express it by using Zero-extension theory.

3.4 Zero Extension Theory

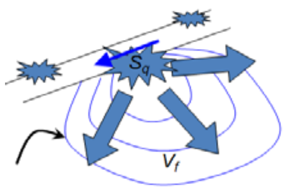

Fig. 4 Moving boundary of flooding/inundating area

Many shallow-water problems could only be formulated correctly by zero depth along a moving boundary that evolved according to the flow characteristics (Bates and Hervouet, 1999). Zero extension theory has been used here to solve a free boundary problem. This theory treats moving boundary with the analytic domain expanded outside (Fig. 4) (Hamaguchi, 1998). Here, a hypothetical domain adjoined to the analytic domain along the boundaries is provided and then that variable is assumed to have a constant value of zero over the hypothetical domain.

3.5 Overflow Model

The discharge that overflows from each stream segment to the flooded area is calculated from the difference between the water level of the channel and the grid section connected to it by assuming Honma's overflow formula of a trapezoid dam is applicable (Mizuyma and Yazawa, 1987). The weir equation depends on whether there is flooding on the surface or not. If the surface is not flooded at the time, then it is calculated as a free flowing weir (Eq. 32) and if the surface is flooded then as a submerged weir (Eq. 33).

$$Q=\mu Bh_1\sqrt{2gh_1} \qquad \text{for } \frac{h_2}{h_1}\le 2/3 \quad (32)$$

$$Q=\eta Bh_2\sqrt{2g(h_1-h_2)} \qquad \text{for } \frac{h_2}{h_1}> 2/3 \quad (33)$$

Where, h_1 and h_2 are water depth u/s and d/s of the bank in relation to the bank crest; B is an overflow width; μ and η are factors for overflow.

4. Data Details

For simulation, hydro-meteorological and geographic data are required. Geographic data such as DEM, land use, boundary data is taken from global database. GCM (Global Climate Models) data has been used for rainfall and temperature. GCM data used here is the super high resolution (20km spatial and hourly temporal) GCM outputs based on A1B scenario of IPCC SRES AR4. AGCM20 has been chosen here to bridge the spatial and temporal resolution gap between the GCMs and hydrologic use. Moreover, it has advantage in simulating orographic rainfall and frontal rain bands. Also it has the advantages of avoiding conventional problem on a spatial scale, not requiring further regional or statistical downscaling (Kim et al., 2009 and Kaoru et al., 2009). GCM data has been used here after bias correction. Observed daily rainfall from sixty five stations for the period of 1979-2000 is used for bias correction for GCM precipitation, while for temperature; observed monthly average temperature from eleven stations for the period of 1996-2000 is used. For the analysis, bias corrected data from the year 1979-2003 has been used. Detail process on data preparation and bias correction can be referred to Sapkota et al., 2010.

5. Results

Fig. 5 shows channel flow simulation using diffusive wave approximation at Hanoi.

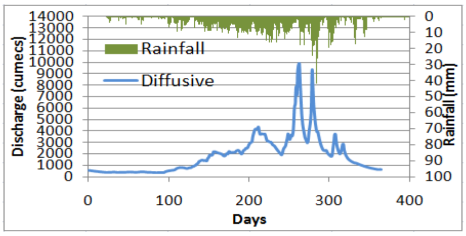

Fig. 5 Channel flow Simulation at Hanoi station

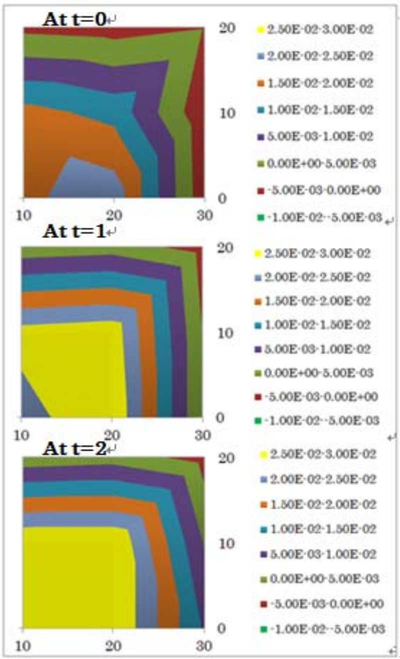

Fig. 6 Surface water head as simulated by flood inundation model

For the verification of the flood inundation model, Hanoi city in Red river basin has been taken. Preliminary simulation results are presented in this paper. Fig.6 and 7 depict the surface water head as simulated by flood inundation model at different time periods. Here the area taken is very coarse (9km by 9km mesh). Though, it can give a glimpse of future calculation.

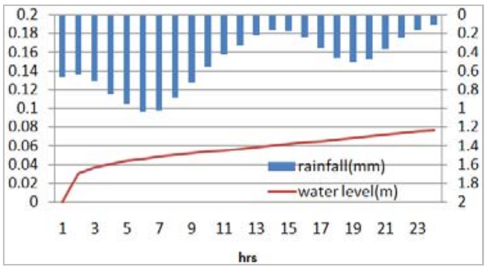

Fig. 7 Surface water head at Hanoi

6. Conclusions

In this study, process of simplified inundation simulation program coupled with rainfall-runoff processes is constructed to simulate flooding. The zero extension theory proposed in this study is relatively a new approach. Proposed model is suitable for flood inundation simulation considering all the components of the hydrologic cycle.

Acknowledgements

The authors are thankful to Global Center for Education and Research on Human Security Engineering for Asian Megacities for supporting this work and the KAKUSHIN Program of the Ministry of Education, Culture, Sports, Science and Technology of Japan (MEXT) for providing the GCM data

References

Bates, P.D. and De Roo, A.P.J. (2000): A simple raster-based model for flood inundation simulation, Journal of Hydrology, pp. 54-77.

Bates, P.D. and Hervouet, J.M. (1999): A new method for moving-boundary hydrodynamic problems in shallow water, Proc. of Royal Society, London, Vol. 455, pp. 3107-3128.

Dutta, D. and Herath, S. (2004): Trends of floods in Asia and Flood Risk Management with Integrated River Basin Approach, Proceedings of the 2nd International Conference of Asia Pacific Hydrology and Water Resources Association, Singapore, Volume I, pp. 55-63.

Hamaguchi, T. (1998): Studies on inverse problems relating to design for underground dam through new modeling for groundwater flow with moving boundaries, Doctoral dissertation, Kyoto University.

Hansson, K. and Ekenberg, L. (2002): Flood Mitigation Strategies for the Red River Delta, Commons in an Age of Globalisation", the Ninth Conference, 2002 - dlc.dlib.indiana.edu

Kaoru, T., Kim, S. Tachikawa, Y. and Nakakita, E. (2009): Assessing Climate Change Impact on Water Resources in the Tone River Basin, Japan, Using Super-High-Resolution Atmospheric Model Output, Journal of Disaster Research Vol. 4, No. 1, pp. 12-23.

Kim, S., Tachikawa, Y., Nakakita, E. and Kaoru, T. (2009): Climate Change Impact on Water Resources Management in the Tone River Basin, Japan, Annuals of Disas. Prev. Res. Inst., Kyoto Univ., No. 52B, pp 587-606.

Kojiri, T., Hamaguchi, T. and Ode, M. (2008): Assessment of global warming impacts on water resources and ecology of a river basin in Japan, J. of Hydro-environment Research, Elsevier, Vol. 1, pp.164-175.

Le, T.P.Q., Garnier, J., Gilles, B., Sylvian, T. and Minh, C.V. (2007): The changing flow regime and sediment load of the Red River, Vietnam. Journal of Hydrology, vol. 334, pp. 199-214.

Mizumaya, T. and Yazawa, A. (1987): Computer simulation of debris flow depositional processes, Erosion and Sedmentation in the Pacific Rim , Proceedings of the Corvallis Symposium, August 1987, IAHS Publ. no. 165.

Piotrowski, J.A. (2010): Development of a High-Resolution Two-Dimensional Urban/Rural Flood Simulation, MS Thesis, University of Iowa.

Sapkota, M., Hamaguchi, T., Sato, Y. and Kojiri, T. (2010): Hydrological Simulations in Red River Basin using Super High Resolution GCM Outputs with Geostatistical Processes, Annuals of Disaster Prevention Research Institute, Kyoto University, No. 53B, pp 675-682.

Tran, V.A., Masumoto, S., Raghavan, V. and Shiono, K. (2007): Spatial Distribution of Subsidence in Hanoi Detected by JERS-1 SAR Interfeormetry, Geoinformatics, vol.18, no.1, pp.3-13.

ハイドロビームを用いたベトナム紅河流域における洪水災害の数値解析

Mukta SAPKOTA*・浜口俊雄・小尻利治

*京都大学大学院工学研究科

要　旨

洪水災害は世界でも最も恐ろしい災害の１つであって，それを減災するために洪水の特徴について信頼できる情報を得ることは重要である。本研究では，洪水特性を解析して湛水地域を特定することで重要情報となるように格子セル単位でハイドロビーム(流域水文環境評価モデル)と結合できる集約化された洪水湛水モデルを開発した。具体的な作業としては，簡略化したナビア・ストークス方程式を集約化し，都市域に適用するには都合の良い湛水伝播モデルを開発した。最後にベトナム紅河を対象としてハノイにおける洪水被害シナリオをシミュレーションし，その湛水変動を確認したところ，湛水の拡がりと水深変化が捉えられており，開発モデルが有効であるとわかった。

キーワード: ハイドロビーム，洪水湛水，移動境界